LA-UR-12-21065
Approved for public release; distribution is unlimited.

Title: Uranium vacancy mobility at the sigma 5 symmetric tilt grain boundary in UO2

Author(s): Uberuaga, Blas P.

Intended for: Report

Uranium vacancy mobility at the Σ5 symmetric tilt grain boundary in UO_2

Blas Pedro Uberuaga
Los Alamos National Laboratory, Los Alamos, NM 87545
(Dated: April 30, 2012)

I. INTRODUCTION

An important consequence of the fissioning process occurring during burnup is the formation of fission products. These fission products alter the thermo-mechanical properties of the fuel. They also lead to macroscopic changes in the fuel structure, including the formation of bubbles that are connected to swelling of the fuel. Subsequent release of fission gases increase the pressure in the plenum and can cause changes in the properties of the fuel pin itself. It is thus imperative to understand how fission products, and fission gases in particular, behave within the fuel in order to predict the performance of the fuel under operating conditions.

Fission gas redistribution within the fuel is governed by mass transport and the presence of sinks such as impurities, dislocations, and grain boundaries. Thus, to understand how the distribution of fission gases evolves in the fuel, we must understand the underlying transport mechanisms, tied to the concentrations and mobilities of defects within the material, and how these gases interact with microstructural features that might act as sinks. Both of these issues have been addressed in previous work under NEAMS [1–3]. However, once a fission product has reached a sink, such as a grain boundary, its mobility may be different there than in the grain interior and predicting how, for example, bubbles nucleate within grain boundaries necessitates an understanding of how fission gases diffuse within boundaries. That is the goal of the present work.

In this report, we describe atomic level simulations of uranium vacancy diffusion in the pressence of a Σ5 symmetric tilt boundary in urania (UO_2). This boundary was chosen as it is the simplest of the boundaries we considered in previous work on segregation and serves as a starting point for understanding defect mobility at boundaries. We use a combination of molecular statics calculations and kinetic Monte Carlo (kMC) to determine how the mobility of uranium vacancies is altered at this particular grain boundary. Given that the diffusion of fission gases such as Xe are tied to the mobility of uranium vacancies, these results given insight into how fission gas mobility differs at grain boundaries compared to bulk urania.

II. METHODS

A. Potential

We use the U-O potential derived by Basak et al [4] for these calculations. It should be noted that there are a number of potentials that have been developed for UO_2. Our choice of the Basak potential is based on our previous experience that it agrees reasonably well with DFT calculations of GB structure. Furthermore, it provides a good description of the elastic constants of UO_2 leading to a more accurate representation of the strain energy. However, all of the UO_2 potentials are limited in their applicability, and none of them are perfect. We expect that the qualitative trends we describe here are independent of the potential, though the details may differ. We also use the Basak potential for all calculations for convenience in comparing results with previous work we have done.

B. Molecular statics

Our approach involves two steps. First, we characterize all of the diffusion pathways (within certain assumptions) for uranium vacancies as a function of position of the vacancy near the grain boundary plane. This is done by first creating a vacancy at every possible site within a simulation cell that contains two Σ5 tilt grain boundaries (see Figure 1) and minimizing the structure. Then, for each of these sites, the neighboring uranium atoms are displaced into the vacancy such that the vacancy moves one nearest neighbor distance in all possible directions. We determine the possible directions by finding all uranium neighbors within a distance of 4 angstroms. In the bulk, this results in 12 nearest neigbor uranium atoms, but near the grain boundary, there are some sites that have 11, 12, or 13 neighbors. These final positions of the vacancy are then minimized. We then have the initial and final positions for the vacancy to hop from each possible site in the system to each possible neighbor. These positions are then used as the starting point for nudged elastic band (NEB) [5] calculations to determine the saddle point for that particular hop. Given

that in our simulation cell there are 480 possible vacancy sites and roughly 12 neighbors per site, this results in 5760 calculations. These calculations give the energy barrier E_m for the vacancy to hop via any of these events.

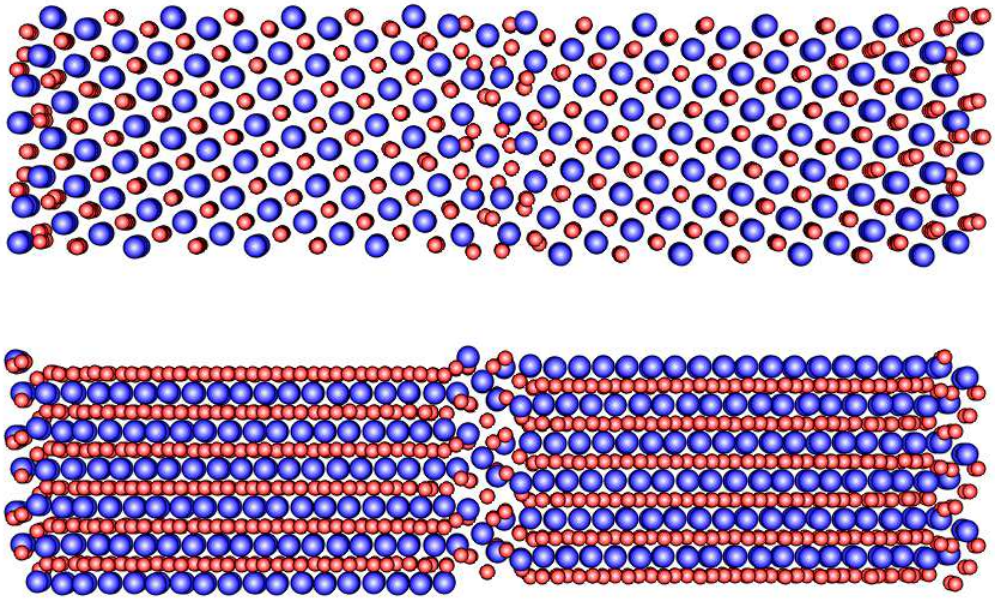

FIG. 1: Structure of the $\Sigma 5$ symmetric tilt grain boundary in UO_2. Top, the view down the tilt axis (along x). Bottom, the view perpendicular to the tilt axis (along y). The blue spheres indicate uranium ions, the red spheres are oxygen ions. There are two grain boundaries in the simulation cell, one in the center and the other at the periodic boundary at the top and bottom of the cell.

Clearly, not all of these events are independent, as a vacancy hop from site i to neighbor j is symmetrically opposite of one from site j to neighbor i. However, by performing this brute force calculation, we have some redundant information to ensure the calculations converged correctly. It turns out that these minimizations were more difficult than initially estimated as minimizing symmetrically equivalent vacancy structures resulted in different energies. Sometimes this was because the minimizer stopped before it was fully minimized (it reach a convergence criterion too early) or because different local arrangements of oxygen resulted in different minima. To ensure that our database of sites and events connecting sites was consistent, whenever we have different energetics for symmetrically equivalent structures, we chose the lowest one for all symmetrically equivalent sites and set the barrier between them at the lowest energy converged NEB value for that set of minima. This might result in some quantitative inaccuracies as the correct path might still not be identified from this procedure, but we expect it will have little effect on the physical trends we report below.

Figure 2 shows the relative formation energy of vacancies near the $\Sigma 5$ tilt boundary. As is clearly evident, the vacancy is strongly attracted to the grain boundary plane. Figure 3 shows the relative saddle energies as a function of the energy difference between the final and intitial minima (ΔE). We see that there are large variations of the saddle energy for any given value of ΔE; that is, there is not a simple relationship between the two (contrary to many assumptions in kinetic Monte Carlo simulations). Even when ΔE 0 – there is little difference in the vacancy energy before and after the hop – the barriers vary by about 6 eV. This shows that the kinetic behavior near the boundary will be a relatively complex competition between a number of different processes.

C. Kinetic Monte Carlo

These results from atomistic calculations are then used as the input for a kinetic Monte Carlo (kMC) simulation in which the vacancy is allowed to hop from uranium lattice site to uranium lattice site. While the lattice is assumed rigid, it's initial structure is identical to that of the starting $\Sigma 5$ tilt boundary structure (again, see Fig. 1). kMC is a stochastic algorithm that is in principle exact if all possible kinetic pathways and their rates are included in the simulation.

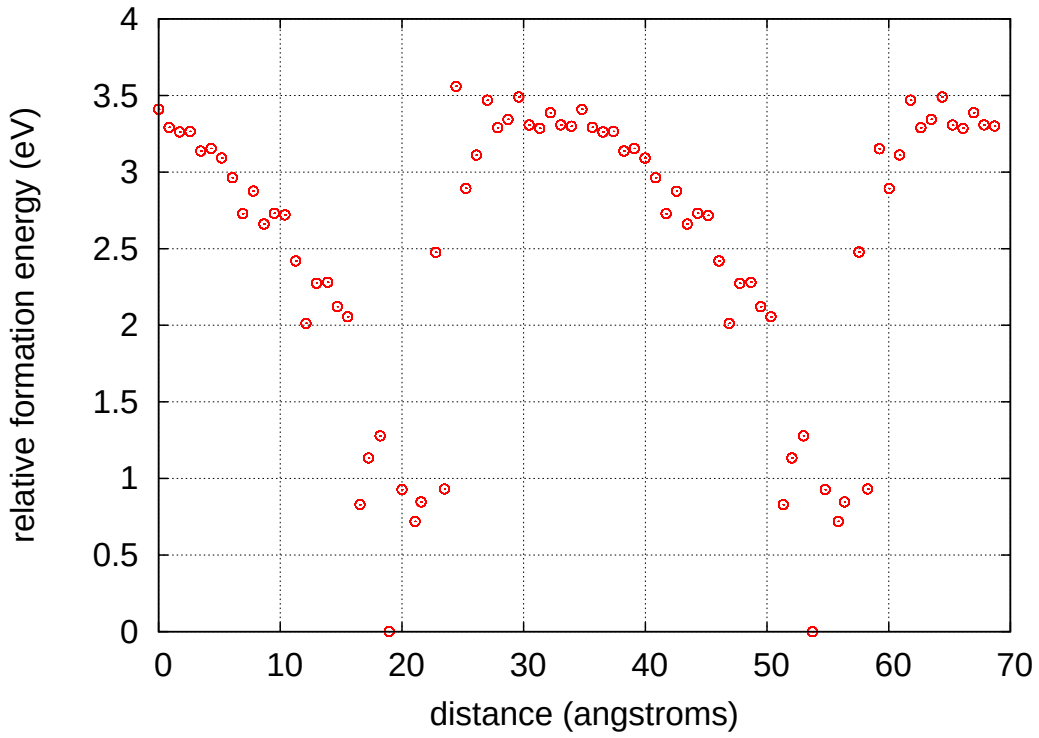

FIG. 2: Relative formation energy of the uranium vacancy as a function of position from the two grain boundary planes.

The rate k_{ij} of a given process taking the vacancy from site i to j is given by $k_{ij} = \nu_{ij} \exp(-E_m^{ij}/k_b T)$ where k_B is the Boltzmann constant and T is temperature. As stated above, E_m^{ij} is directly obtained from the atomistic simulations. In principle, ν could so be derived as well, but calculating ν_{ij} is a computationally expensive task and is a relatively minor contributor to differences in k for different processes, which is typically dominated by E_m^{ij} (residing within the exponential). Thus, here we assume $\nu_{ij} = 10^{13}$/s for all i and j.

Given the rate catalog defined by k_{ij}, a kMC simulation proceeds as follows. For the current position i of the vacancy, all of the possible hops are identified, and the total rate $k_i^{total} = \sum_{j=1}^{N} k_{ij}$ where N is the toal number of neighboring positions for this vacancy. One of these events is then chosen at random, weighted by its relative rate: k_{ij}/k_i^{total}. The time for the event is correspondingly calculated via the equation $\Delta t = ln(1/s)/k_i^{total}$, where s is a random number between 0 and 1, and added to the total simulation time. The vacancy is moved into the chosen neighboring site and the steps repeated. The simulations are run for 5 million kMC steps.

By monitoring the mean square displacement (MSD) during the course of the simulation, we can measure the diffusivity of the defect: $\langle r^2 \rangle \sim Dt$, where r is the MSD of the particle or collection of particles in the simulation over a time t. The D that results from this equation is not exactly the diffusion constant as measured by experiment as we have a constant defect concentration in our simulations while the defect concentration in experiment varies with temperature. Thus, we are extracting the mobility per defect of the uranium vacancy. In the simulations reported here, we have only one vacancy within the simulation cell. However, in principle, more defects can be added with a simple rule for their interaction (that they simply block one another). In this way, we can get first order effects on defect-defect interactions on defect mobility. Future work will look at this effect.

In the measurements of defect diffusion reported here, we averaged over 10 simulations at each temperature considered. For each simulation, there are error bars for the extracted diffusivity D; here, those are ignored. Rather, we report error bars related to the standard error associated with the D averaged over the 10 simulations.

As the grain boundary is highly anisotropic, with faster diffusion along the tilt axis than perpendicular to it, the mobilities along the tilt axis (along x in our coordinate system) will be very different than along y, the direction perpendicular to the tilt axis. We thus measure mobilities both along x and along y to determine the relative mobilities, or anisotropies in diffusion, in the two dimensions.

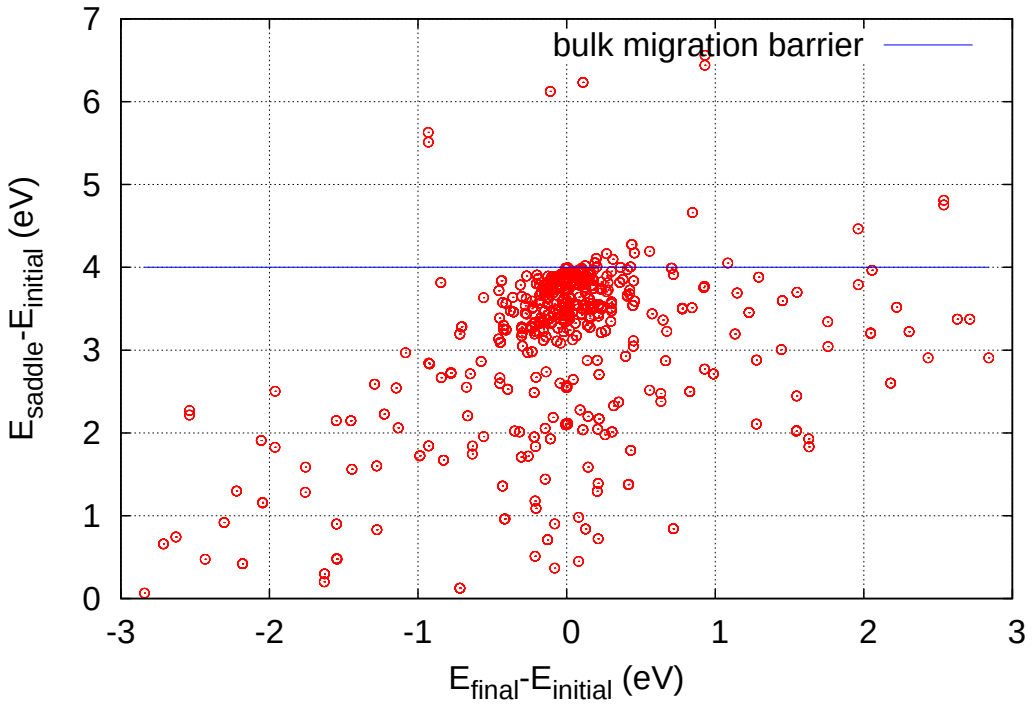

FIG. 3: Relative saddle energies as a function of the difference in energy between the final and initial state of the event. While there is a rough correlation, it is certainly not linear, as often assumed. For any given difference in energy, there are a range of saddle energies, up to 6 eV in some cases.

III. RESULTS

Figure 4 shows example trajectories at four different temperatures. As is clearly evident, as the temperature is increased from 2500K to 10,000K, the diffusive behavior of the vacancy changes from 1D to 2D within the grain boundary plane. The total time for these simulations ranges from 0.5 to 5 μs. This is not such a great difference, considering the wide range of temperatures, but this is because the rate for the fastest processes is very similar, a consequence of the low barriers associated with them.

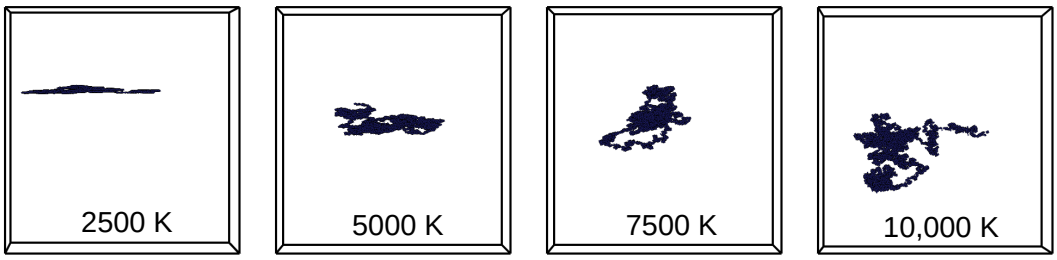

FIG. 4: Example trajectories at each temperature considered (2500K, 5000K, 7500K, and 10,000K). There is a clear transition from one-dimensional to two-dimensional motion as the temperature is increased.

A note about the temperatures is in order. Clearly, these are physically meaningless temperatures, as urania melts at temperatures approaching 3000K. However, even with the advantages provided by kMC, we are unable to simulate long enough times at operating temperatures to see diffusive behavior. Thus, we raise the temperature to artificially high values to extract trends in diffusivity as a function of temperature to extrapolate to lower temperatures of interest.

Given trajectories such as those illustrated in Fig. 4, we then measure D as described above. The results are presented in Fig. 5 for diffusion both in the x and y dimensions (parallel and perpendicular to the tilt axis). Even at

the artificially high temperature of 10,000K, there is still significant differences in the mobility of the vacancy along x compared to along y. This difference only increases with decreasing temperature. The ratio of D along x vs along y is shown in Fig. 6. This ratio increases from a factor of about 2 at 10,000K to a factor of about 400 at 2500K. If we imagine extrapolating to 1000K, the relative anisotropy factor would increase to nearly 10^7 (based on a linear extrapolation of Fig. 6).

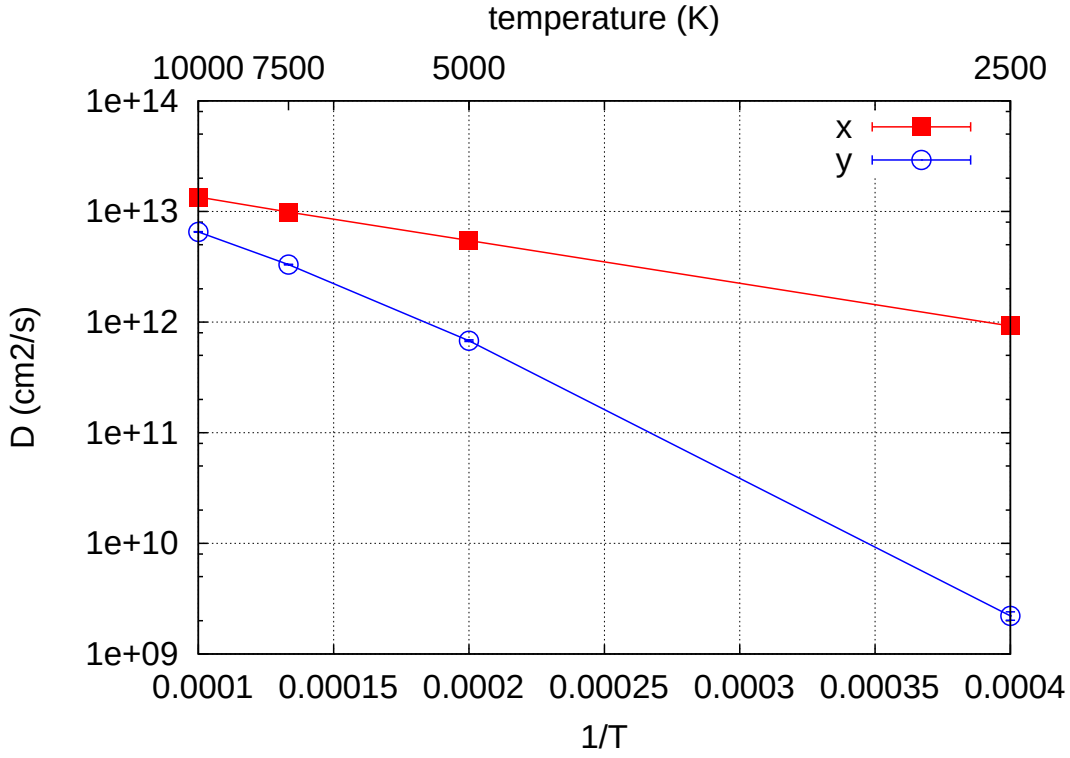

FIG. 5: Diffusivity of the uranium vacancy within the grain boundary plane, both in along the tilt axis (x) and perpendicular to it (y). Diffusivity is much higher along the tilt axis than perpendicular to it.

We can understand this behavior by looking at the saddles that connect the various sites at the grain boundary plane. This is shown in Fig. 7. We see that, along the tilt axis, there is a set of low energy sites (black circles) that are connected by relatively lower barriers (smaller than 1 eV). No such pathway exists along y, perpendicular to the tilt axis. The smallest barrier that takes the vacancy all the way along the y dimension to a new equivalent position and could describe net transport is roughly 2 eV or so.

We can also extract the effective migration energies of vacancies directly from the diffusivities presented in Fig 5 by fitting the results to an Arrhenius expression $D = D_0 \exp(-E_m/k_B T)$. Doing so, we find effective migration energies of E_m^x 0.8 eV and E_m^y 2.1 eV, consistent with the rough estimate made by looking at the saddle landscape in Fig. 7. It is interesting that both of these migration energies are significantly lower than the bulk migration energy predicted by this potential of 4 eV. At any temperature at which bulk migration is active, diffusion in both x and y will be active. However, diffusion along x will be so much faster that the vacancy will likely reach any strong sink (triple junction or line junction between grains, surfaces, or bubbles) via this 1D mechanism long before diffusion along y occurs.

Another feature that can be observed in Fig. 5 is that, while the diffusivity along x is Arrhenius over the temperature range considered, the same is not true along y. There is a clear bend in the curve. Often, such a trend indicates anharmonic effects in the migration barrier, but that is explicitly not possible in these simulations as every rate is treated, by definition, as harmonic. Thus, this is an indicator that as the temperature varies, different barriers are becoming important. This must be due to a multiplicity effect for higher barriers: while they are of higher energy, there are more of them, so they can start to be more important at high temperatures than the lower barriers. We will investigate this further in future work.

A final note about temperatures should be made. This potential over-predicts the migration barrier for uranium vacancies in bulk UO_2 by about 0.4 eV compared to density functional theory (DFT) calculations [1, 2]: 4.0 eV with the potential vs 3.6 eV with DFT. Thus, the temperatures at which this potential would predict uranium vacancy

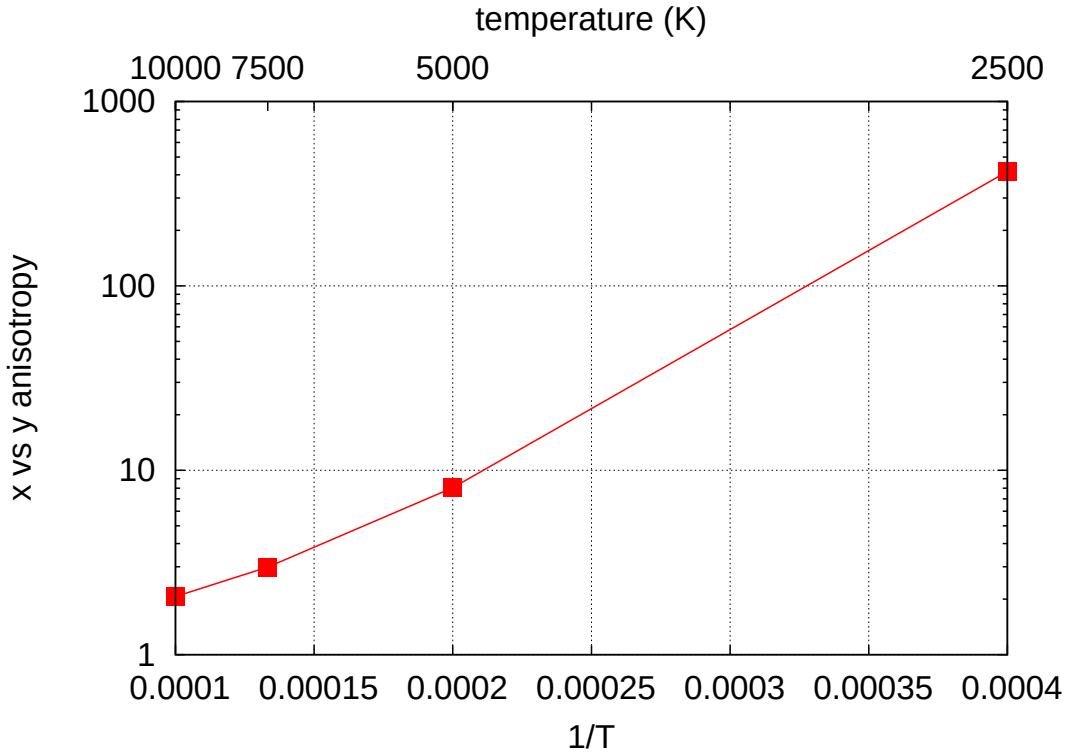

FIG. 6: Anisotropy in x vs y diffusivities as a function of temperature. As the temperature is decreased, the anisotropy grows very quickly (note that it is a log scale).

mobility to become active say on the 1 second time scale would be higher than that predicted by DFT. However, this difference would only be slightly higher. If we can assume that all barriers in the system, even those at the grain boundary, scale by a similar ratio, we would estimate that the temperature at which mobility of uranium vacancies at the grain boundary becomes active would shift from 285K to 255K, based again on diffusion on a 1 second time scale. Similarly, the temperature at which mobility in the y direction would becomes active would shift from 750K to 675K. Bulk diffusion is active on the 1 second time scale at temperatures of 1430K with the potential result and 1285K with the DFT result.

IV. DISCUSSION AND CONCLUSIONS

Previous work by other groups has found that, in some situations, defects can actually exhibit less mobility at grain boundaries than in the bulk [6]. This is because there are often deep trap states at grain boundaries that are not directly connected to other low energy states and thus, for diffusion, the defect has to escape the trap first. This is clearly not occurring for the $\Sigma 5$ symmetric tilt grain boundary studied here. Rather, along the tilt axis, there is a string of low energy sites connected to one another via which the uranium vacancy can easily diffuse. Even in the direction perpendicular to the tilt axis, diffusion is faster than in the bulk. This higher mobility, combined with the fact that there will be a higher concentration of uranium vacancies at the grain boundary than in the bulk (due to the lower energies of formation there) means that mass transport at the $\Sigma 5$ tilt grain boundary will be significantly higher than in the bulk. Thus, once Xe makes its way to this boundary, it will quickly diffuse along the grain boundary to find other sinks, such as other Xe. The consequence is that this boundary, at least, will not likely directly act as a nucleation site for Xe bubbles or, stated another way, nucleation of Xe bubbles at this boundary will likely require significantly more Xe than in the bulk as the mobility is so much higher.

To this point, we have studied only one grain boundary in UO_2. The goal is to study a set of grain boundaries and determine how sensitive defect mobility is to grain boundary structure. To this end, we will next investigate a $\Sigma 5$ twist grain boundary. Based on what we have learned about this problem in our study of the $\Sigma 5$ tilt boundary, we will approach the next boundary in a more efficient manner. We will only consider unique pathways in the calculation of NEBs rather than doing all of them brute force. This will allow us to do the next boundary much more quickly.

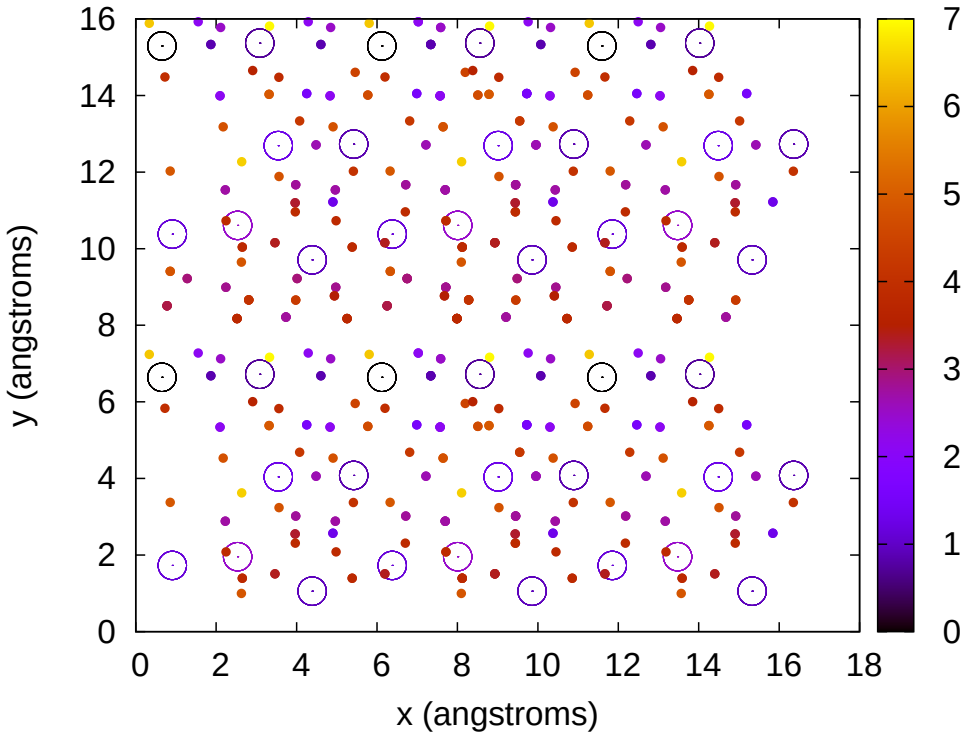

FIG. 7: Schematic of the saddles connecting the various stable uranium vacancy sites at and near the grain boundary plane. The large open circles are stable sites while the small filled circles represent the saddles connecting them (placed exactly half way between sites). The colors of both types of circles indicate the energy of teh site or saddle. There is a low barrier path way along x, the tilt axis, leading to fast diffusion along that dimension. In contrast, no such pathway exists along y.

However, we will take extra care to ensure that all calculations are converged. We thus expect the next boundary to take significantly less time than this first one did. That said, for more complex boundaries, such as random boundaries where there are no symmetries between sites, we will not be able to reduce the number of calculations. It is not yet clear if we will be able to afford performing all of the calculations on such a boundary.

Another aspect we will explore in the coming months is the role of defect concentration at the grain boundary on defect mobility. We will implement a simple blocking model that forbids migration of vacancies to sites where another vacancy already resides. This is not exactly what happens in real UO_2, but it will give us a first order estimate of how transport will vary as more defects are introduced.

To conclude, we have examined the mobility of the uranium vacancy, as it pertains to Xe transport, at the $\Sigma 5$ tilt grain boundary. We find that the mobility of the vacancy is significantly higher at the grain boundary than in the bulk. This is true for both dimensions within the grain boundary plane. However, the mobilty along the tilt axis is much higher than perpendicular, meaning that effectively diffusion under operating conditions will be one-dimensional. This will have ramifications for mesoscale models of fission gas evolution as the transport of fission gas along grain boundaries will depend on the orientation of the grains within the material.

V. ACKNOWLEDGMENTS

The authors are grateful to D. A. Andersson and C. R. Stanek for helpful discussions. This work was sponsored by the Nuclear Energy Advanced Modeling and Simulation (NEAMS) program.

[1] B. Dorado, et al. Physical Review B, in press.
[2] D. A. Andersson, et al. Physical Review B 84, 54105 (2011).
[3] P. Nerikar, et al. Physical Review B 84, 174105 (2011).

[4] C. B. Basak, A. K. Sengupta, and H. S. Kamath, J. Alloys Compd. 360, 210 (2003).
[5] G. Henkelman, B. P. Uberuaga, and H. Jnsson, J. Chem. Phys. 113, 9901 (2000).
[6] A. Pedersen and H. Jonsson, Acta Mat. 57, 4036 (2009).